NEUROPATHOLOGY

Neuropathology 2014; **34**, 1–10 doi:10.1111/neup.12052

Original Article

Neuronal differentiation associated with Gli3 expression predicts favorable outcome for patients with medulloblastoma

Hiroaki Miyahara,[1,3] Manabu Natsumeda,[2] Junichi Yoshimura,[2] Ryosuke Ogura,[2] Kenichi Okazaki,[1] Yasuko Toyoshima,[1] Yukihiko Fujii,[2] Hitoshi Takahashi[1] and Akiyoshi Kakita[1]

Departments of [1]Pathology and [2]Neurosurgery, Brain Research Institute, University of Niigata, Niigata and [3]Department of Pediatrics and Child Neurology, Oita University Faculty of Medicine, Oita, Japan

Medulloblastoma (MB) is a malignant cerebellar tumor arising in children, and its ontogenesis is regulated by Sonic Hedgehog (Shh) signaling. No data are available regarding the correlation between expression of Gli3, a protein lying downstream of Shh, and neuronal differentiation of MB cells, or the prognostic significance of these features. We re-evaluated the histopathological features of surgical specimens of MB taken from 32 patients, and defined 15 of them as MB with neuronal differentiation (ND), three as MB with both glial and neuronal differentiation (GD), and 14 as differentiation-free (DF) MB. Gli3-immunoreactivity (IR) was evident as a clear circular stain outlining the nuclei of the tumor cells. The difference in the frequency of IR between the ND+GD (94.4%) and DF (0%) groups was significant ($P < 0.001$). The tumor cells with ND showed IR for both Gli3 and neuronal nuclei. Ultrastructurally, Gli3-IR was observed at the nuclear membrane. The overall survival and event-free survival rates of the patients in the ND group were significantly higher than those in the other groups. The expression profile of Gli3 is of considerable significance, and the association of ND with this feature may be prognostically favorable in patients with MB.

Key words: desmoplastic/nodular, Gli3, medulloblastoma, neuronal differentiation, prognosis, sonic hedgehog.

Correspondence: Akiyoshi Kakita, MD, PhD, Department of Pathology, Brain Research Institute, University of Niigata, 1 Asahimachi, Chuo-ku, Niigata 951-8585, Japan. Email: kakita@bri.niigata-u.ac.jp

Received 10 April 2013; revised 11 June 2013 and accepted 12 June 2013; published online 29 July 2013.

INTRODUCTION

Medulloblastoma (MB) is a malignant, invasive tumor of the cerebellum, predominantly affecting children. According to the WHO classification of CNS tumors,[1] MB corresponds to grade IV, and is subdivided histopathologically into four types: classic MB (CMB), desmoplastic/nodular MB (DNMB), MB with extensive nodularity (MBEN), and anaplastic/large cell MB. Several clinicopathological studies have provided evidence that the prognosis of patients with MB depends on the histological tumor type. For example, the survival period for patients with anaplastic/large cell MB is shorter than that for patients with CMB.[2–7] Patients with MBEN are expected to have a better outcome than patients with other types.[8,9] On the other hand, it is still unclear whether DNMB-type histology predicts a favorable outcome. Several investigations have indicated that patients with DNMB survive longer than those with CMB;[10–16] however, others have provided evidence to the contrary.[16,17]

A recent breakthrough in understanding the pathomechanisms of MB has been the discovery of the Sonic Hedgehog (Shh) signaling pathway. Shh is considered to regulate growth and patterning during development of the cerebellum,[18] and plays an essential role in the tumorigenesis of a subset of MB.[19,20] Moreover, Shh plays an integral role in a wide variety of developmental processes in vertebrates, and in the development of carcinomas in various organs (Fig. 1A,B). The Shh ligand binds to patched (PTCH) receptors, and inhibits activity against Smoothened on the cytoplasmic membrane. In the on-state, Gli1 and Gli2, the Gli activators in mammals, are produced in the cytoplasm and transported into the nucleus, where various target oncogenes against Shh,

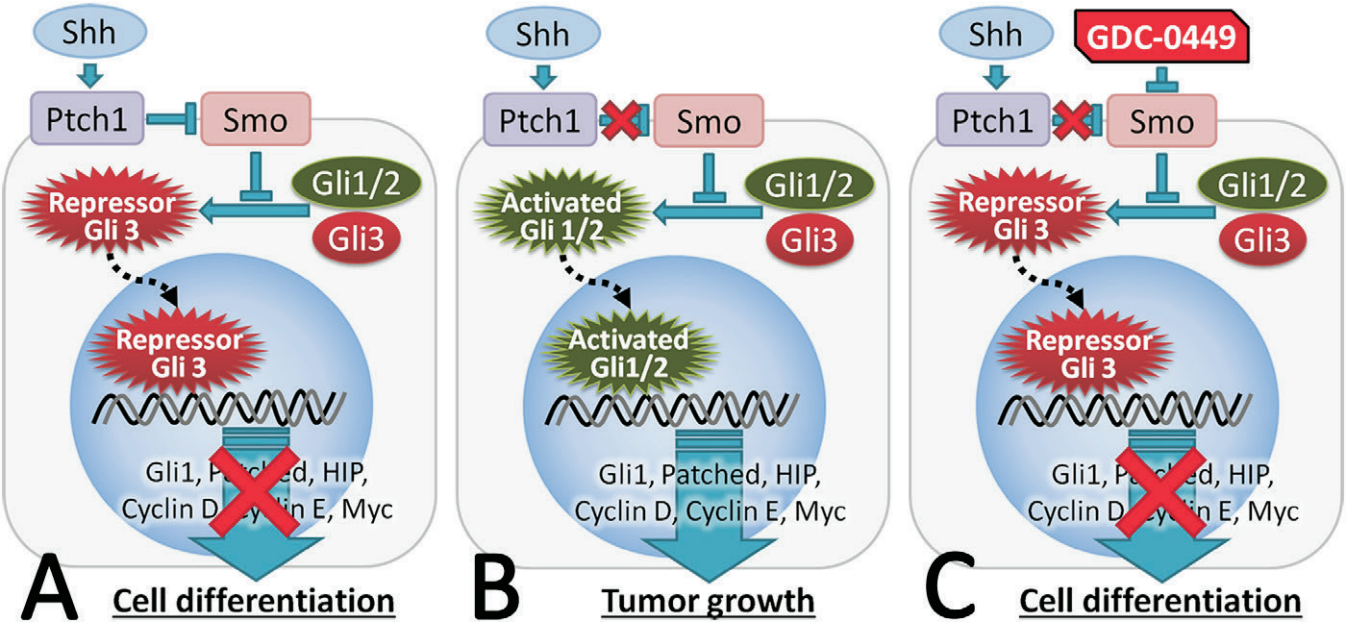

Fig. 1 Sonic hedgehog (Shh) pathway and cell differentiation. Shh ligand binds to patched receptors (PTCH1), inhibiting activity against Smoothened (Smo) on the cytoplasmic membrane. (A) In the off-state, Gli3 repressor (Gli3-Rep) is produced in the cytoplasm and transported into the nucleus, where Gli3-Rep inhibits the transcription of target oncogenes and promotes normal differentiation. (B) In the on-state, Gli1 and Gli2 activator (Gli1/2-Act) is produced and transported into the nucleus, and target oncogenes against Shh are transcribed. (C) GDC-0449, a Shh pathway inhibitor, drives normal differentiation through the regulation of Gli3.

including Cyclin D, Cyclin E, Myc, Gli1 and PTCH, are transcribed (Fig. 1B). In the off-state, by contrast, a Gli repressor, Gli3, is produced in the cytoplasm and transported into the nucleus,[21] where it inhibits transcription of the target oncogenes and promotes normal differentiation (Fig. 1A).

It is still unclear whether the expression of the Shh signaling pathway influences the differentiation of MB cells, and consequently affects the outcome of patients with MB. The present study attempted to determine whether expression of Gli3 contributes to neuronal differentiation of the tumor cells and to a favorable outcome for patients with MB.

MATERIALS AND METHODS

Patients

We reviewed the medical records of 32 consecutive patients (19 males, 13 females: age at onset, mean ± SD = 9.7 ± 5.8 years) with pathologically confirmed MB who were referred to the Brain Research Institute, University of Niigata, Japan, between 1982 and 2010. All the patients had undergone maximum possible tumor resection, followed by 30.6 to 36.0 Gy of craniospinal irradiation with a 18.0–23.4 Gy posterior fossa boost. Patients ($n = 6$: five male, one female: age 8.2 ± 7.2 years) who were admitted to our hospital between 1982 and 1991 had received radiotherapy only. On the other hand, a large proportion of the patients included in the present study ($n = 23$: 12 males, 11 females: age 9.8 ± 4.8 years), who were admitted between 1992 and 2007, had undergone radiotherapy followed by adjuvant chemotherapy with regimens of carboplatin and either etoposide or ifosfamide, but otherwise in combination with cisplatin and etoposide. In the more recent period between 2008 and 2010, patients ($n = 3$: two male, one female: age 12.4 ± 10.5 years) had undergone radiotherapy, high-dose chemotherapy with cisplatin, cyclophosphamide and vincristine, and peripheral blood stem cell transplantation. A summary of the clinical profiles of the patients, including age at onset, sex, risk evaluation factors as proposed by Laurent *et al.*,[22] tumor location, and post-surgical radiochemotherapy regimens, is shown in Table 1. None of the patients had a family history of neurological diseases or specific carcinomas.

CMB showed a sheet-like arrangement of densely packed cells with round-to-oval or carrot-shaped hyperchromatic nuclei surrounded by scant cytoplasm (Fig. 2A). DNMB was characterized by a nodular arrangement of highly proliferative cells with hyperchromatic nuclei (Fig. 2B), and intercellular reticulin fiber networks. Twenty-two patients (14 male, eight female: age 10.5 ± 6.1 years) and 10 patients (five male, five female: age 8.1 ± 4.9 years) showed features of CMB and DNMB, respectively. There

Table 1 Clinicopathological profiles of the 32 patients with medulloblastoma

	n	10-year survival rate			
		OS		EFS	
		% ± SD	*P*	% ± SD	*P*
Age at onset					
≤7 years	11	73 ± 13	ns	73 ± 13	ns
>7 years	21	67 ± 11		48 ± 11	
Sex					
Male	19	74 ± 10	ns	68 ± 11	*
Female	13	62 ± 14		38 ± 13	
Risk‡					
Average risk	14	78 ± 11	ns	71 ± 12	ns
High risk	18	61 ± 11		50 ± 12	
Tumor location					
Vermis	30	67 ± 09	–	60 ± 09	ns
Hemisphere	2	100 ± 0		50 ± 35	
Chemoradiation					
CSI only (I)	6	50 ± 20	†	50 ± 20	
CSI+ICE/PE (II)	23	70 ± 10		52 ± 10	ns
CSI+HDCx+PBSCT (III)	3	100 ± 0		67 ± 27	
Histology					
Classic	21	62 ± 11	ns	52 ± 11	*
Desmoplastic/nodular	11	82 ± 12		82 ± 12	
Ki-67 labeling index					
<10%	13	62 ± 14		62 ± 13	
10–50%	14	79 ± 11	ns	57 ± 13	ns
>50%	5	60 ± 22		60 ± 22	
GLI-3 immunoreactivity					
Positive	12	83 ± 11	ns	83 ± 11	**
Negative	20	60 ± 11		45 ± 11	

CSI, craniospinal irradiation; HDCx, cisplatin, cyclophosphamide and vincristine; ICE, carboplatin and etoposide or ifosfamide; ns, not significant; PBSCT, peripheral blood stem cell transplantation; PE, cisplatin and etoposide. *$P \leq 0.1$, **$P < 0.05$, †(I)–(II): ns, (II)–(III): $P < 0.001$, (I)–(III): $P < 0.05$. ‡Risk evaluation proposed by Laurent *et al.*[22]

were no specimens showing myogenic or melanotic differentiation, or features of anaplastic/large cell MB.[1,4]

Next, we divided the present 32 patients with MB into three groups on the basis of the differentiated features of the tumor cells: neuronal differentiation (ND), glial and neuronal differentiation (GD) and differentiation-free (DF) groups. On the basis of the following criteria,[1] we defined tumor cells as having features of ND: a reduced nuclear–cytoplasmic ratio, a fibrillary matrix and uniform cells with a neurocytic appearance, negligible mitotic activity (Fig. 2C,D) and immunoreactivity for neuron-specific markers such as neuronal nuclei (NeuN: Fig. 2E) and doublecortin (DCX: Fig. 2F). Moreover, we defined tumor cells as having features of GD on the basis of immunoreactivity for GFAP. Specimens taken from one patient (a 1-year-old boy) showed extensive nodules with remarkable ND, and these features were compatible with those of MBEN.[8,9] We included this case in the ND group. Therefore, we included 15 patients (10 male, five female: age 7.9 ± 4.0 years) and three patients (two male, one female: age 4.8 ± 5.0 years) in the ND and GD groups, respectively. The DF group was defined by the absence of both ND and GD ($n = 14$, eight male, six female: age 11.7 ± 6.6 years).

Histological and immunohistochemical procedures

The surgical specimens were fixed with 20% buffered formalin and embedded in paraffin. Histological examination was performed on 4-μm-thick sections stained with HE and silver impregnation for reticulin. The paraffin-embedded sections were also immunostained by the avidin-biotin-peroxidase complex method (Vector, Burlingame, CA, USA) with diaminobenzidine as the chromogen. Primary antibodies against the following antigens were used: NeuN (monoclonal, clone A60; Chemicon, Temecula, CA, USA; 1:150), DCX (polyclonal; Abcam, Cambridge, UK; 1:2000, pretreated by heating), GFAP (polyclonal; Dako, Glostrup, Denmark; 1:4000), Gli3 (polyclonal; Santa Cruz Biotechnology, Santa Cruz, CA, USA; 1:800, pretreated by heating) and Ki-67 (monoclonal, clone MIB-1; Dako; 1:100, pretreated by heating). The Ki-67 labeling index was evaluated by determining the percentage of positive nuclei present in at least 1000 tumor cells in representative areas of the specimens.

A double-labeling immunofluorescence study was performed on sections using the rabbit polyclonal Gli3 antibody and either the mouse monoclonal NeuN antibody or a mouse monoclonal GFAP antibody (clone GA5; Chemicon; 1:400). The secondary antibodies used were Alexa Fluor 488 goat anti-rabbit IgG (Molecular Probes, Eugene, OR, USA; 1:1000) and Alexa Fluor 568 goat anti-mouse IgG (Molecular Probes; 1:1000). Vectashield DAPI (Vector) was used as a nuclear marker. A laser scanning confocal microscope (Carl Zeiss LSM510, ver. 4.0, Göttingen, Germany) equipped with a ×40 oil immersion objective was used to visualize immunoreactivity.

Immunoelectron microscopy

The ultrastructural localization of Gli3 was examined using surgical specimens taken from two patients with MB (ND: one; GD: one), by employing the post-embedding method previously described.[23] Small tissue blocks of the tumors were prepared from the formalin-fixed tissue, and washed with PBS. Then, the tissue blocks were washed with gradually increasing concentrations of dimethylformamide, and embedded in LR White resin (London Resin Company, Berkshire, UK). Ultrathin sections were cut, incubated with Gli3 (1:20) for 36 h, and reacted with 15-nm gold colloidal particle-conjugated anti-rabbit IgG (British BioCell, Cardiff, UK; 1:30). The sections were then stained with lead citrate, and examined with a Hitachi H-7100 electron microscope at 75 kV.

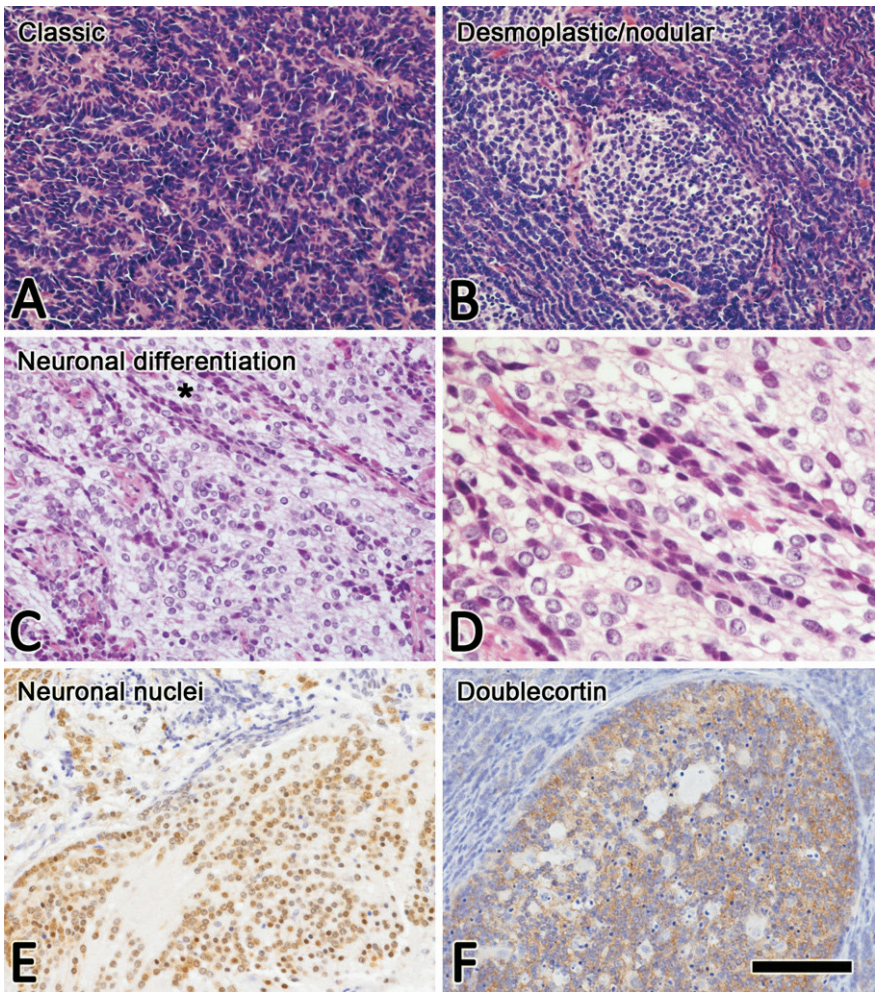

Fig. 2 Representative histopathological features of the specimens. (A) Classic medulloblastoma (MB) showing a sheet-like arrangement of densely packed cells with hyperchromatic nuclei and scant cytoplasm. (B,C) Desmoplastic/nodular MB (DNMB). The tumor cells form nodules separated by desmoplastic septa. (B) DNMB without apparent features of neuronal differentiation. (C) MB with neuronal differentiation (ND group), showing relatively loosely arranged tumor cells with vesicular nuclei and fine processes. (D) A higher-magnification view of the area indicated by an *asterisk* in (C) demonstrating a biphasic pattern of the tumor cells with neuronal differentiation and those with more immature features with hyperchromatic nuclei. (E,F) Immunohistochemical features of ND cases. The nuclei and cytoplasm of neuronal differentiated cells are reactive for neuronal nuclear antigen (NeuN) (E) and doublecortin (F), respectively. (A–D) HE staining. Scale bar: 100 μm for (A–C,E,F) and 50 μm for (D).

Statistical analysis

The overall survival (OS) and event-free survival (EFS) rates of each group after initial clinical presentation were estimated using the method of Kaplan and Meier. Death, disease progression, recurrence and secondary malignancy were considered as the events. Statistical significance of differences between survival curves was tested by means of the log-rank test. Tests for associations between different parameters were carried out by the chi-squared test for 2×2 and 2×3 contingency tables. Data analysis was carried out using the SPSS version 17.0 software package (SPSS Inc., Chicago, IL, USA).

RESULTS

Gli3 expression

Gli3 immunoreactivity (IR) was observed as a clear circular stain outlining the nucleus of the tumor cells (Fig. 3A,B). The IR was observed in a large proportion of the ND+GD cases (94.4%: 17/18), but none of the DF cases (0%: 0/14). The difference in frequency of IR cases between the groups was significant ($P < 0.001$) (Fig. 5 and Table 2).

In the ND and GD cases, the majority of the tumor cells within the nodules appeared to show neuronal differentiation with IR for both Gli3 and NeuN (Fig. 3A,B). A double immunofluorescence study demonstrated that circular Gli3-IR enclosed densely packed granular NeuN-IR in the nuclei (Fig. 3C–H). In the GD cases, we observed a small number of Gli3-IR nuclei and GFAP-IR cytoplasmic processes of the tumor cells within and around the nodules (Fig. 3I–M).

In both ND and GD cases, immunoelectron microscopy demonstrated Gli3-IR at the inner membrane of the nuclear envelope with nuclear chromatin nearby, and inside the nucleus (Fig. 4).

Prognosis

Several clinical and histological characteristics, including age at onset, sex, risk evaluation factors proposed by Laurent *et al.*,[22] histological type, Ki-67 labeling index, and

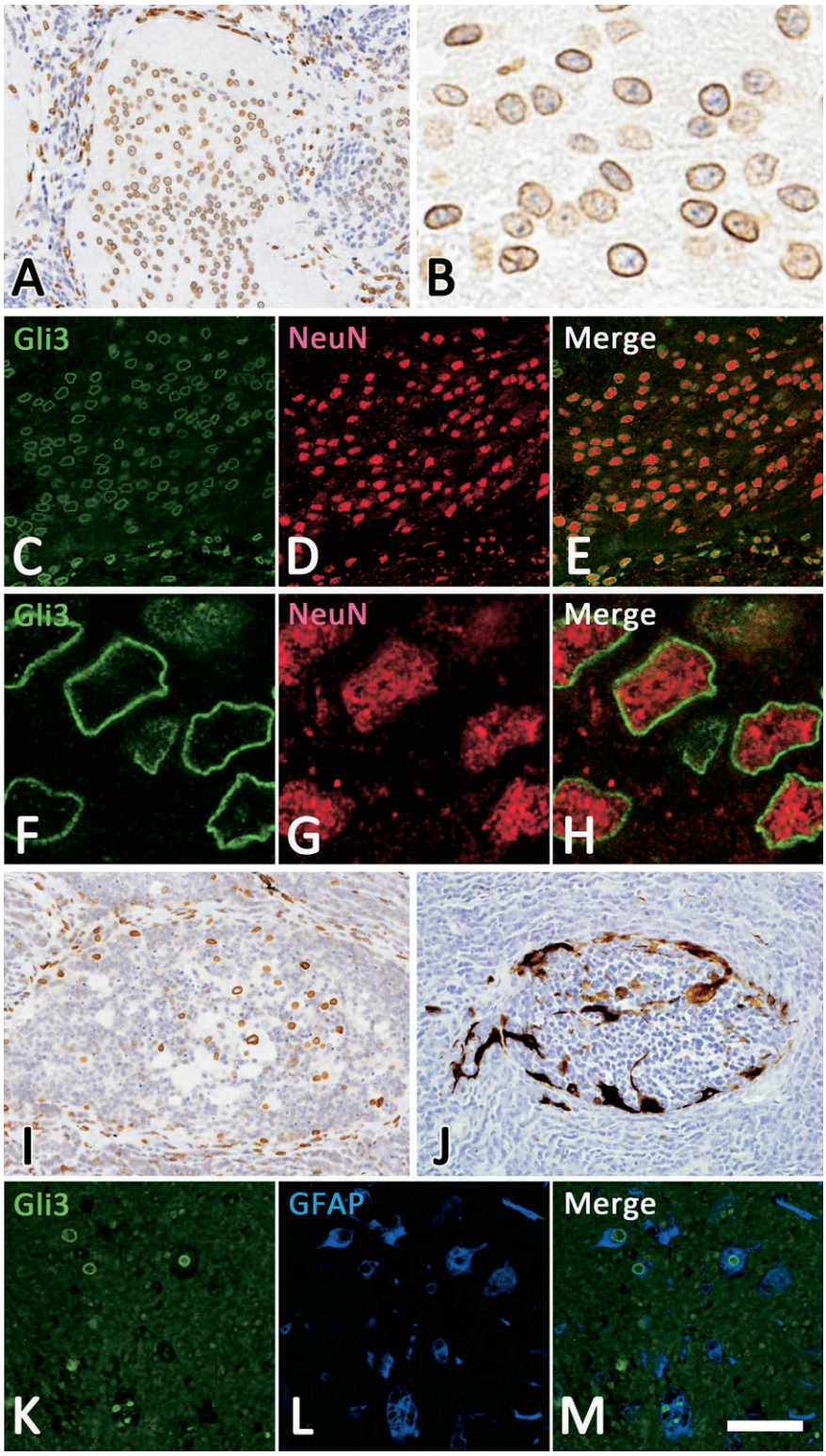

Fig. 3 Immunohistochemical features. (A–H) Tumor cells in cases from the neuronal differentiation (ND) group. (A) The nuclei of neuronal differentiated cells within the nodules are reactive for Gli3. Note that nuclei of many cells around the nodules are unreactive for Gli3. (B) Higher-magnification view of Gli3-positive cells. Gli3-immunoreactivity is observed as a clear circular stain outlining the nucleus of the tumor cells. (C–H) Immunofluorescence with the Gli3 (*green*) and neuronal nuclear antigen (NeuN) (*red*) signals to demonstrate the spatial relationship of the two antigens. (C–E) Low-power views. (F–H) Higher-power views. (E,H) Merged image of both signals. A large proportion of the nuclei are reactive for both Gli3 and NeuN. The circular Gli3 signal encloses the densely packed granular NeuN signal. (I–M) Tumor cells in a case from the glial differentiation (GD) group. (I,J) A small number of nuclei of the tumor cells within the nodule are reactive for Gli3 (I), and those within and at the periphery of the nodule are reactive for GFAP: (J). (K–M) Immunofluorescence with the Gli3 (*green*: K) and GFAP (*blue*: L) signals for demonstrating the spatial relationship of the two antigens. (M) Merged image of both signal. Some cells are reactive for both Gli3, as the circular stain around the nucleus, and GFAP in their cytoplasm, but some are reactive for either alone (M). Scale bar: 82 µm for (A,B,I,J), 50 µm for (C–E,K–M), and 6 µm for (F–H).

Gli3-IR, showed no significant relationship with the OS rate, whereas induction of chemoradiation was significantly correlated with longer OS (Table 1). With regard to EFS rate, Gli3-IR in the tumor was significantly ($P < 0.05$) associated with a favorable patient outcome. Being male and having DNMB tended to be associated with a favorable outcome, but not to a significant degree ($P < 0.1$) (Table 1).

Evaluation of differences in the profiles of each histopathological group is summarized in Table 2. Both the OS and EFS rates in the ND group were significantly

Table 2 Comparison of profiles in each of the groups

Subgroups	Total	DF	Differentiation			Statistical verdict			
			All	ND	GD				
		A	B	C	D	A-B	A-C	A-D	C-D
Number	32	14	18	15	3	–	–	–	–
Age at onset									
≤7 years	11	4	7	6	1	ns	ns	ns	ns
>7 years	21	10	11	9	2				
Sex									
Male	19	8	11	10	1	ns	ns	ns	ns
Female	13	6	7	5	2				
Tumor location									
Vermis	30	13	17	15	2	ns	ns	ns	ns
Hemisphere	2	1	1	0	1				
Risk†									
Average risk	14	6	8	8	0	ns	ns	ns	ns
High risk	18	8	10	7	3				
Chemoradiation									
CSI only	6	4	2	1	1	ns	ns	ns	ns
CSI+ICE/PE	23	15	8	6	2				
CSI+HDCx+PBSCT	3	2	1	0	1				
10-year survival rate (%)									
OS	69 ± 8	50 ± 13	83 ± 9	87 ± 9	67 ± 27	**	**	ns	ns
EFS	63 ± 9	43 ± 13	78 ± 10	80 ± 10	33 ± 27	**	***	ns	**
Pathology									
Classic	22	13	9	7	2	**	**	ns	ns
Desmoplastic/nodular	10	1	9	8	1				
Ki-67 labeling index									
<10%	13	5	8	7	1	ns	ns	ns	ns
10–50%	14	5	9	7	2				
>50%	5	4	1	1	0				
GLI-3 immunoreactivity									
Positive	17	0	17	14	3	***	***	**	ns
Negative	15	14	1	1	0				
Positivity rate (%)	53	0	94	93	100	–	–	–	–

CSI, craniospinal irradiation; DF, differentiation-free; DN, desmoplastic/nodular; EFS, event-free survival; GD, neuronal and glial differentiation; HDCx, cisplatin, cyclophosphamide and vincristine; ICE, carboplatin and etoposide or ifosfamide; ND, neuronal differentiation; ns, not significant; OS, overall survival; PBSCT, peripheral blood stem cell transplantation; PE, cisplatin and etoposide. $^{**}P < 0.05$, $^{***}P < 0.001$. †Risk evaluation proposed by Laurent *et al.*[22]

higher than those in the other groups (Fig. 6 and Table 2). The GD group showed outcomes as equally poor as those of the DF group. It was found that the Ki-67 labeling index in the DF group tended to be higher than those in the ND and GD groups, although the inter-group differences were not significant (Table 2).

DISCUSSION

The findings of this study indicated that neuronal differentiation is associated with Gli3 expression in MB cells, and that this feature predicts a favorable outcome for patients with MB.

In the present study, all patients in the ND group showed a favorable course (Fig. 6 and Table 2). Previous reports have indicated that patients with MB accompanied by neuronal differentiation[24,25] and those with MBEN[8,9] show good progress, being consistent with our findings. On the other hand, the association between glial differentiation in the tumor and patient prognosis has been unclear; the three patients in the GD group (Fig. 3I–M) showed miserable courses (Table 2), whereas some previous reports have indicated that patients with MB showing glial differentiation progressed well.[24,25]

Some previous reports have indicated that patients with DNMB did not show significant longer survival than those with CMB.[16,17] Consistent with this, the difference on the 10-year OS rates of patients with CMB and those with DNMB was not significant (Table 2). Apparently, a large proportion of DNMB cases exhibited features of neuronal differentiation and Gli3 expression (Table 2). Therefore, combination of desmoplastic/nodular histological characteristics, NeuN indicating neuronal differentiation, and Gli3 expression, is useful for predicting a favorable outcome.

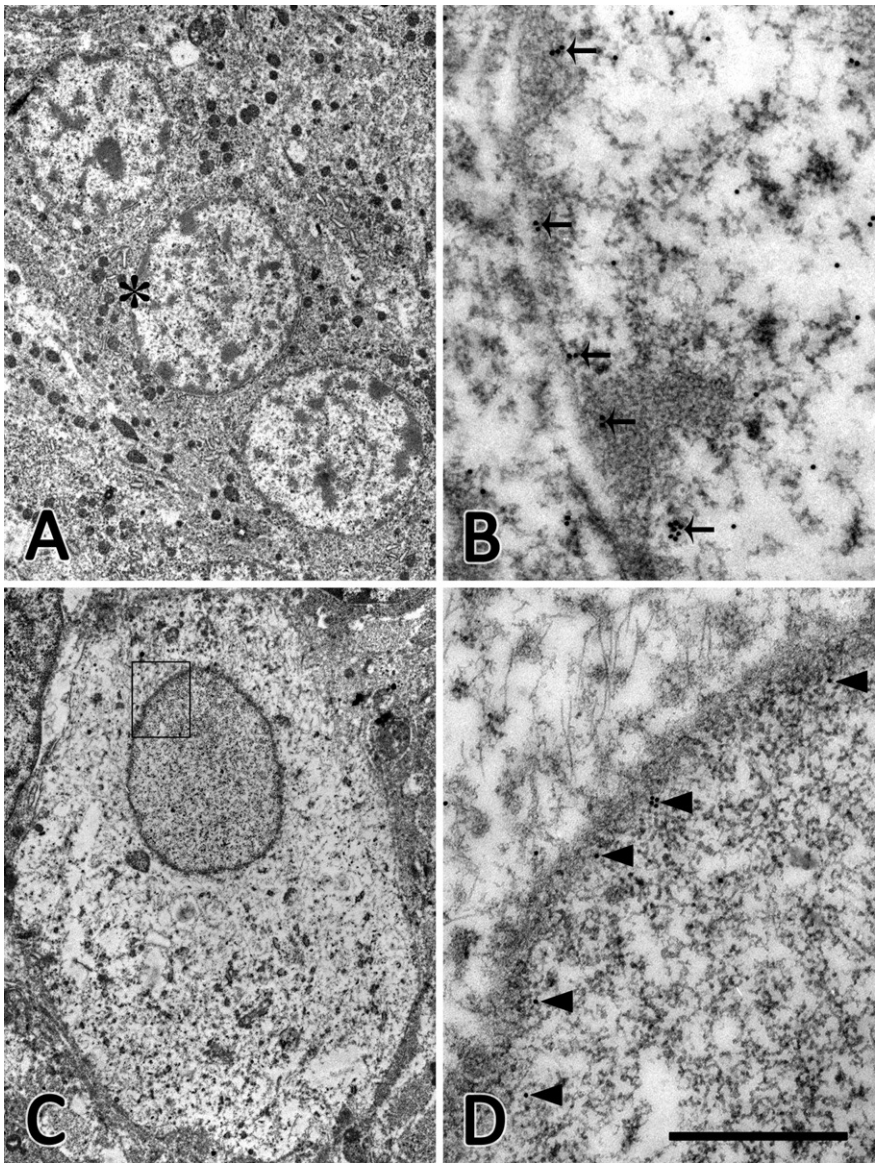

Fig. 4 Ultrastructural localization of Gli3. Immunoelectron microscopy of tumor cells within the nodules of neuronal differentiation (ND) and glial differentiation (GD) cases. Gli3 is visualized using 15-nm immunogold particles. (A) A low-magnification view showing several chromatin aggregates in the nucleus, and mitochondria, ribosomes and other organelles in the perinuclear cytoplasm. (C) A low-magnification view showing a relatively homogeneous inner structure of the nucleus and many glial fibrils in the plump cytoplasm. (B,D) A higher-magnification view of the area indicated by the *asterisk* in (A) and the *clear square* in (C), demonstrating Gli3 at the inner membrane of the nuclear envelope and nuclear chromatin nearby (arrows and arrowheads). Scale bar = 5 µm for (A), 7.5 µm for (C), and 615 nm for (B,D).

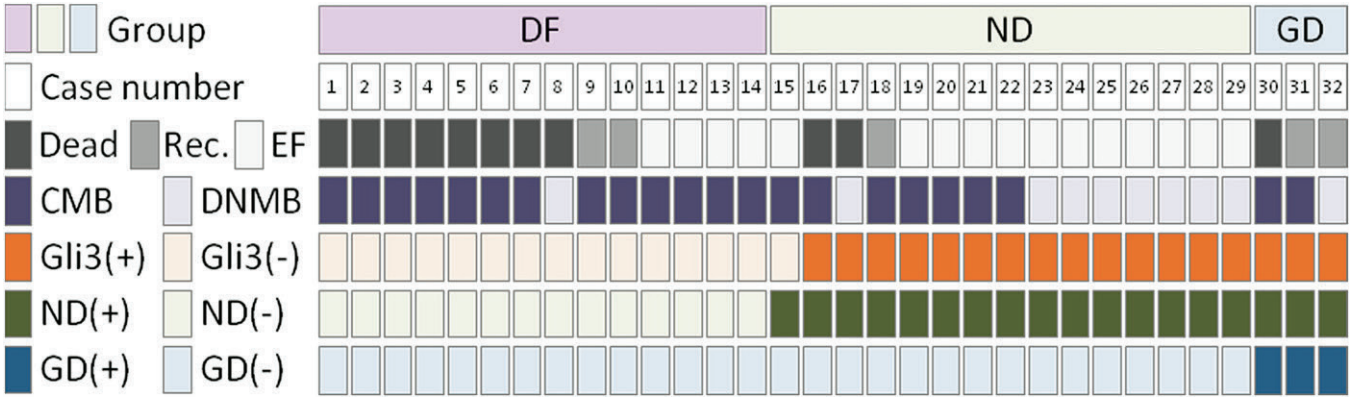

Fig. 5 Summary of medulloblastoma (MB) cases. Neuronal differentiation is well correlated with Gli3 expression in MB cells. Histopathologically, differentiation-free (DF) cases tend to show CMB. The DF and GD groups included many cases that were fatal or recurred. ND: Neuronal differentiation, GD: Glial differentiation, Rec.: Recurrence, EF: Event free, CMB: Classic MB, DNMB: Desmoplastic/nodular MB. , Group; , Case number; , Dead; , Rec.; , EF; , CMB; , DNMB; , Gli3(+); , Gli3(–) , ND(+); , ND(–); , GD(+); , GD(–).

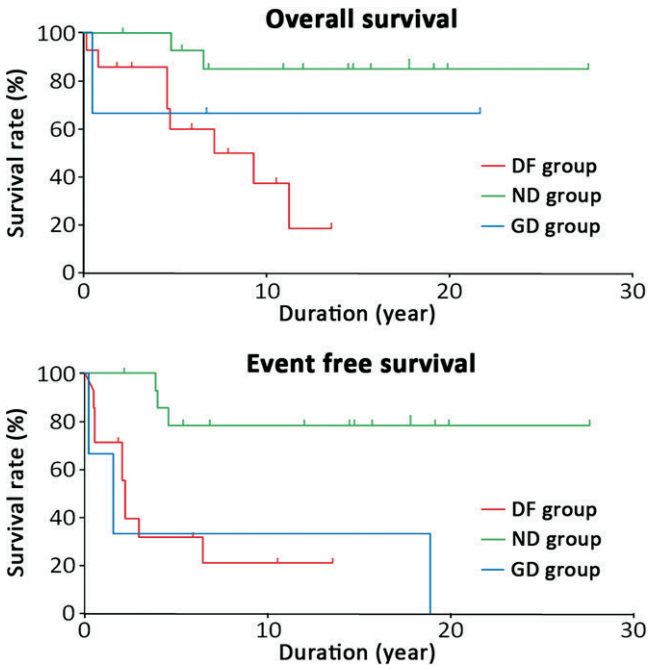

Fig. 6 Actuarial survival curves for patients with medulloblastoma (MB). Overall survival rate (A) and event-free survival rate (B) for patients in the differentiation-free (DF), neuronal differentiation (ND), and glial differentiation (GD) groups are shown. All patients in the ND group are alive without recurrence. Both of the rates for patients in the ND group are significantly higher than those for patients in the DF and GD groups. —, DF group; —, ND group; —, GD group.

One of the striking findings of this study was the clear topographical correlation between neuronal differentiation and Gli3 expression (Fig. 3A,B). We also confirmed the neuronal character of individual Gli3-expressing cells using NeuN immunohistochemistry (Fig. 3C–H). Thus, activation of the Shh signaling pathway involving Gli3 influences the neuronal differentiation of MB cells. Concerning the Shh pathway, mutations in the *PTCH* gene have been detected in 20–40% of DNMB cases,[26,27] suggesting the importance of the pathway in tumor histogenesis.

Recently, a study involving administration of GDC-0449, a Shh antagonist (Fig. 1C), to a patient with MB and *PTCH1* mutation was performed.[28] Although the patient had multiple metastatic lesions, the tumors showed rapid regression after this treatment.[28] This therapeutic approach has been verified by another recent study.[12] Thus, regulation of this pathway affects tumorigenesis in MB.

As well as in MB,[12] roles for Shh in the development of other CNS tumors, such as glioblastoma and neuroblastoma,[20] as well as of carcinomas arising in visceral organs such as the colon,[29] and also the breast,[30] have been reported. Further investigation of patients with such tumors will be needed to clarify the correlation between Gli3 expression and patient prognosis.

Besides the Shh signaling pathway, molecular biological investigations and large-scale clinical studies have shown that various factors influence the prognosis of patients with MB. For example, expression of the downstream protein β-catenin promoted by the Wnt signaling pathway is considered to predict a favorable clinical course in children with MB.[31] In the present study, we did not include results of immunohistochemistry for β-catenin/CTNNB1. In our series of medulloblastoma a subset of tumor cells exhibited nuclear staining; however, simultaneously we also observed unreliable cytoplasmic staining with or without nuclear staining. On the other hand, amplification of MYCC/MYCN,[6] Bcl-2[32] and ErbB2[33] in tumor cells is thought to be an adverse prognostic factor. However, it has also been proposed that expression of Bcl-2 may lead to a favorable outcome.[9] Being male,[17] and the presence of metastatic lesions at the time of initial clinical presentation,[2,34] may be associated with an undesirable course. Cellular characteristics such as apoptotic[5] and mitotic activity,[7,35] as indicated by the Ki-67[36–38] and BrdU[39] labeling indices, may also suggest tumor progression. Thus, combinations of clinical, histopathological and molecular features may be used to predict more precisely the outcome of individual patients with MB. However, in the present study we detected no significant factors, including age, sex or the Ki-67 labeling index, that eventually influenced the outcome of patients with MB (Tables 1 and 2), although this may have reflected the small number of cases examined.

Recent genomic, transcriptome and DNA methylomics profiling approaches have suggested the existence of four distinct molecular subgroups of MB: wingless (WNT), SHH, Group 3 and Group 4.[40–43] It has been anticipated that molecular profiling of biomarkers could be used for prognostication of patients with MB. Immunohistochemistry is one of the conventional approaches for verifying the expression of target proteins characterizing each subtype. Therefore, sets of candidate proteins, for example secreted fizzled-related protein 1 (SFRP1) and Gli1 for the SHH subgroup, CTNNB1 and DKK1 for the WNT subgroup, NPR3 for Group C, and KCNA1 for Group D, have been introduced.[40,41] We have tried immunohistochemistry with antibodies against these introduced proteins for assignment of the subgroups,[41] but failed to obtain reliable labeling (data not shown). In addition to immunohistochemistry, a molecular profiling study would be needed for such subgroup assignment. Based on the findings of the present study, Gli3 could be a potentially reliable and immunohistochemically informative prognostic biomarker for patients with MB.

The interesting expression profile of Gli3 (Fig. 3) may imply a certain biological role of the protein in MB cells, but its significance has remained unclear. It seems unlikely

that the Gli3-expression could be associated with the cell cycle, because Gli3-immunoreactivity and Ki-67 labeling index in each group (Table 2) showed no apparent correlation. The ultrastructural localization of the protein (Fig. 4) appeared consistent with its immunohistochemical pattern. It is known that Gli3 is transported from the cytoplasm into the nucleus, where it inhibits transcription of target oncogenes.[21] However, its expression profile has not been fully explained, even when considering its function. It has been shown that lamin A, a functional protein that maintains the shape of the nuclear envelope of muscle cells, is expressed as a similar circular stain around the nucleus.[44] At present, there are no data suggesting an association between Gli3 and lamin A.

In summary, our findings indicate that neuronal differentiation associated with Gli3 expression contributes to a favorable outcome in patients with MB. This information may be of importance when considering new therapeutic strategies for MB.

ACKNOWLEDGMENT

This work was supported by a grant (24-7) for Nervous and Mental Disorders and a Health Labor Science Research Grant from the Ministry of Health, Labor and Welfare, Japan.

REFERENCES

1. Giangaspero F, Eberhart CG, Haapasalo H, Pietsch T, Wiestler OD, Ellison DW. Medulloblastoma. In: Louis DN, Ohgaki H, Wiestler OD, Cavenee WK, eds. *WHO Classification of Tumours of the Central Nervous System*, 4th edn. Lyon: IARC, 2007; 132–140.
2. Brown HG, Kepner JL, Perlman EJ *et al*. "Large cell/anaplastic" medulloblastomas: a Pediatric Oncology Group Study. *J Neuropathol Exp Neurol* 2000; **59**: 857–865.
3. Eberhart CG, Kepner JL, Goldthwaite PT *et al*. Histopathologic grading of medulloblastomas: a Pediatric Oncology Group study. *Cancer* 2002; **94**: 552–560.
4. Giangaspero F, Rigobello L, Badiali M *et al*. Large-cell medulloblastomas. A distinct variant with highly aggressive behavior. *Am J Surg Pathol* 1992; **16**: 687–693.
5. Giangaspero F, Wellek S, Masuoka J, Gessi M, Kleihues P, Ohgaki H. Stratification of medulloblastoma on the basis of histopathological grading. *Acta Neuropathol* 2006; **112**: 5–12.
6. Lamont JM, McManamy CS, Pearson AD, Clifford SC, Ellison DW. Combined histopathological and molecular cytogenetic stratification of medulloblastoma patients. *Clin Cancer Res* 2004; **10**: 5482–5493.
7. McManamy CS, Lamont JM, Taylor RE *et al*. Morphophenotypic variation predicts clinical behavior in childhood non-desmoplastic medulloblastomas. *J Neuropathol Exp Neurol* 2003; **62**: 627–632.
8. Giangaspero F, Perilongo G, Fondelli MP *et al*. Medulloblastoma with extensive nodularity: a variant with favorable prognosis. *J Neurosurg* 1999; **91**: 971–977.
9. Suresh TN, Santosh V, Yasha TC *et al*. Medulloblastoma with extensive nodularity: a variant occurring in the very young – clinicopathological and immunohistochemical study of four cases. *Childs Nerv Syst* 2004; **20**: 55–60.
10. Bailey CC, Gnekow A, Wellek S *et al*. Prospective randomised trial of chemotherapy given before radiotherapy in childhood medulloblastoma. International Society of Paediatric Oncology (SIOP) and the (German) Society of Paediatric Oncology (GPO): SIOP II. *Med Pediatr Oncol* 1995; **25**: 166–178.
11. Chatty EM, Earle KM. Medulloblastoma. A report of 201 cases with emphasis on the relationship of histologic variants to survival. *Cancer* 1971; **28**: 977–983.
12. Ellison DW. Childhood medulloblastoma: novel approaches to the classification of a heterogeneous disease. *Acta Neuropathol* 2010; **120**: 305–316.
13. McManamy CS, Pears J, Weston CL *et al*. Nodule formation and desmoplasia in medulloblastomas – defining the nodular/desmoplastic variant and its biological behavior. *Brain Pathol* 2007; **17**: 151–164.
14. Muller W, Afra D, Schroder R, Slowik F, Wilcke O, Klug N. Medulloblastoma: survey of factors possibly influencing the prognosis. *Acta Neurochir (Wien)* 1982; **64**: 215–224.
15. Sure U, Berghorn WJ, Bertalanffy H *et al*. Staging, scoring and grading of medulloblastoma. A postoperative prognosis predicting system based on the cases of a single institute. *Acta Neurochir (Wien)* 1995; **132**: 59–65.
16. Verma S, Tavare CJ, Gilles FH. Histologic features and prognosis in pediatric medulloblastoma. *Pediatr Dev Pathol* 2008; **11**: 337–343.
17. Meurer RT, Martins DT, Hilbig A *et al*. Immunohistochemical expression of markers Ki-67, NeuN, synaptophysin, p53 and HER2 in medulloblastoma and its correlation with clinicopathological parameters. *Arq Neuropsiquiatr* 2008; **66**: 385–390.
18. Dahmane N, Ruiz i Altaba A. Sonic hedgehog regulates the growth and patterning of the cerebellum. *Development* 1999; **126**: 3089–3100.
19. Kimura H, Stephen D, Joyner A, Curran T. Gli1 is important for medulloblastoma formation in Ptc1+/– mice. *Oncogene* 2005; **24**: 4026–4036.

20. Shahi MH, Lorente A, Castresana JS. Hedgehog signalling in medulloblastoma, glioblastoma and neuroblastoma. *Oncol Rep* 2008; **19**: 681–688.
21. Krauss S, Foerster J, Schneider R, Schweiger S. Protein phosphatase 2A and rapamycin regulate the nuclear localization and activity of the transcription factor GLI3. *Cancer Res* 2008; **68**: 4658–4665.
22. Laurent JP, Chang CH, Cohen ME. A classification system for primitive neuroectodermal tumors (medulloblastoma) of the posterior fossa. *Cancer* 1985; **56**: 1807–1809.
23. Tan CF, Yamada M, Toyoshima Y *et al*. Selective occurrence of TDP-43-immunoreactive inclusions in the lower motor neurons in Machado-Joseph disease. *Acta Neuropathol* 2009; **118**: 553–560.
24. Burger PC, Grahmann FC, Bliestle A, Kleihues P. Differentiation in the medulloblastoma. A histological and immunohistochemical study. *Acta Neuropathol* 1987; **73**: 115–123.
25. Katsetos CD, Herman MM, Frankfurter A *et al*. Cerebellar desmoplastic medulloblastomas. A further immunohistochemical characterization of the reticulin-free pale islands. *Arch Pathol Lab Med* 1989; **113**: 1019–1029.
26. Ng D, Stavrou T, Liu L *et al*. Retrospective family study of childhood medulloblastoma. *Am J Med Genet A* 2005; **134**: 399–403.
27. Pietsch T, Waha A, Koch A *et al*. Medulloblastomas of the desmoplastic variant carry mutations of the human homologue of Drosophila patched. *Cancer Res* 1997; **57**: 2085–2088.
28. Rudin CM, Hann CL, Laterra J *et al*. Treatment of medulloblastoma with hedgehog pathway inhibitor GDC-0449. *N Engl J Med* 2009; **361**: 1173–1178.
29. Alinger B, Kiesslich T, Datz C *et al*. Hedgehog signaling is involved in differentiation of normal colonic tissue rather than in tumor proliferation. *Virchows Arch* 2009; **454**: 369–379.
30. ten Haaf A, Bektas N, von Serenyi S *et al*. Expression of the glioma-associated oncogene homolog (GLI) 1 in human breast cancer is associated with unfavourable overall survival. *BMC Cancer* 2009; **9**: 298.
31. Fattet S, Haberler C, Legoix P *et al*. Beta-catenin status in paediatric medulloblastomas: correlation of immunohistochemical expression with mutational status, genetic profiles, and clinical characteristics. *J Pathol* 2009; **218**: 86–94.
32. Das P, Puri T, Suri V, Sharma MC, Sarkar C. Medulloblastomas: a correlative study of MIB-1 proliferation index along with expression of c-Myc, ERBB2, and anti-apoptotic proteins along with histological typing and clinical outcome. *Childs Nerv Syst* 2009; **25**: 825–835.
33. Shim KW, Joo SY, Kim SH, Choi JU, Kim DS. Prediction of prognosis in children with medulloblastoma by using immunohistochemical analysis and tissue microarray. *J Neurosurg Pediatr* 2008; **1**: 196–205.
34. Packer RJ, Sutton LN, Elterman R *et al*. Outcome for children with medulloblastoma treated with radiation and cisplatin, CCNU, and vincristine chemotherapy. *J Neurosurg* 1994; **81**: 690–698.
35. Gilbertson RJ, Jaros E, Perry RH, Kelly PJ, Lunec J, Pearson AD. Mitotic percentage index: a new prognostic factor for childhood medulloblastoma. *Eur J Cancer* 1997; **33**: 609–615.
36. Miralbell R, Tolnay M, Bieri S *et al*. Pediatric medulloblastoma: prognostic value of p53, bcl-2, Mib-1, and microvessel density. *J Neurooncol* 1999; **45**: 103–110.
37. Ohta T, Watanabe T, Katayama Y *et al*. TrkA expression is associated with an elevated level of apoptosis in classic medulloblastomas. *Neuropathology* 2006; **26**: 170–177.
38. Schiffer D, Cavalla P, Migheli A *et al*. Apoptosis and cell proliferation in human neuroepithelial tumors. *Neurosci Lett* 1995; **195**: 81–84.
39. Ito S, Hoshino T, Prados MD, Edwards MS. Cell kinetics of medulloblastomas. *Cancer* 1992; **70**: 671–678.
40. Northcott PA, Korshunov A, Witt H *et al*. Medulloblastoma comprises four distinct molecular variants. *J Clin Oncol* 2011; **29**: 1408–1414.
41. Taylor MD, Northcott PA, Korshunov A *et al*. Molecular subgroups of medulloblastoma: the current consensus. *Acta Neuropathol* 2012; **123**: 465–472.
42. Cho YJ, Tsherniak A, Tamayo P *et al*. Integrative genomic analysis of medulloblastoma identifies a molecular subgroup that drives poor clinical outcome. *J Clin Oncol* 2011; **29**: 1424–1430.
43. Schwalbe EC, Williamson D, Lindsey JC *et al*. DNA methylation profiling of medulloblastoma allows robust subclassification and improved outcome prediction using formalin-fixed biopsies. *Acta Neuropathol* 2013; **125**: 359–371.
44. Pugh GE, Coates PJ, Lane EB, Raymond Y, Quinlan RA. Distinct nuclear assembly pathways for lamins A and C lead to their increase during quiescence in Swiss 3T3 cells. *J Cell Sci* 1997; **110** (Pt 19): 2483–2493.